ORIGINAL ARTICLE

Radio-sensitizing potential of artesunate is mediated by targeting stemness and hypoxia markers in solid Ehrlich tumor implanted in mice

Mohamed I. Morsi¹, Sanaa A. El-Benhawy¹, Samar S. Elblehi², Osama O. Almesrati³, Amal R.R. Arab^{4*}

- ¹Radiation Sciences Department, Medical Research Institute, Alexandria University, Alexandria, Egypt
- ²Pathology Department, Faculty of Veterinary Medicine, Alexandria University, Alexandria, Egypt
- ³Diagnostic & Therapeutic Radiology Department, Faculty of Medical Technology, Misrata, Libya
- ⁴Applied Medical Chemistry Department, Medical Research Institute, Alexandria University, Alexandria, Egypt.

ABSTRACT

Background: Despite the development of various treatment strategies, cancer remains the main cause of death worldwide. Aim: The purpose of this study was to investigate the antitumor effects and radio sensitizing effect of artesunate in combination with ionizing radiation (IR) on the Ehrlich solid carcinoma (ESC). Material and Methods: This study included 8 groups, each included 8 ESC bearing mice. Group I: untreated ESC bearing mice as a control group. Group II: Mice were irradiated with a single dose of irradiation (IR, 6Gy). Group III: Mice treated with artesunate alone (50mg/kg/day). Group IV: Mice treated with the combination of a single dose of IR (6Gy) and artesunate (50mg/kg/day). Group V: Mice treated with artesunate alone (100 mg/kg/day). Group VI: Mice treated with the combination of single dose of IR (6Gy) and artesunate (100 mg/kg/day). Group VII: Mice treated with artesunate alone (200mg/kg/day). Group VIII: Mice treated with the combination of single dose of IR (6Gy) and artesunate (200mg/kg/day). The levels of CD44, ALDH1A1, VEGF and HIF-1- α in tissue homogenate were measured by ELISA. P53 was measured using Immunohistochemistry. Results: Tumor inhibition rate increased, and tumor volume decreased in ESC, indicating that artesunate possesses anti-proliferative effects. Artesunate induced apoptosis through increasing p53 expression. Combination of artesunate with IR significantly elevated tumor damage induced by ionizing radiation. Artesunate induces hypoxia and increases CSC makers in a dose dependent manner. Conclusion: High dose of artesunate could be used as a potent anti-tumor agent against ESC with radio-sensitizing effects through induction of apoptosis. Artesunate induces hypoxia which leads to increased CSCs markers.

Keywords: Artesunate, ALDH1A1, CD44, Ehrlich solid tumor, Ionizing radiation

Editor-in-Chief: Prof. M.L. Salem, PhD - Article DOI: 10.21608/jcbr.2025.291546.1355

ARTICLE INFO

Article history

Received: July 11, 2024 Revised: June 29, 2025 Accepted: July 24, 2025

Correspondence to

Amal R.R. Arab

Applied Medical Chemistry Department Medical Research Institute Alexandria University Alexandria, Egypt. Email: amal_rifaat@yahoo.com

Copyright

©2025 Mohamed I. Morsi, Sanaa A. El-Benhawy, Samar S. Elblehi, Osama O. Almesrati, Amal R.R. Arab. This is an open-access article distributed under the Creative Commons Attribution License, which permits unrestricted use, distribution, and reproduction in any format provided that the original work is properly cited.

INTRODUCTION

Cancer is a multifaceted disease characterized by uncontrolled growth of cells and the dissemination of these abnormal cells in the body (Seigel et al., 2020). Radiotherapy, whether postoperative radiotherapy or neoadjuvant radiotherapy is highly recommended for up to 50% of patients (Jiang et al., 2018). The direct and indirect effects of ionizing radiation determine the efficacy of radiotherapy (Xu., 2022). Radiotherapy aims to shrink tumors and kill cancer cells. Despite radiotherapy's effectiveness in treating cancer in many possible ways, it is often unavoidable that such radiation will cause harmful damage to the surrounding healthy or normal cells. Consequently, it would be preferable to achieve a proper balance between tumor elimination and minimizing probable side effects. The radiosensitizer is a magic bullet to solve this challenge (Goswami et al., 2017). Using a radiosensitizer is an efficient way to boost the killing power of radiation against the tumor, dramatically decreasing the received dosage and limiting the possible damage to normal tissues (Zhang et al., 2015). Worldwide, artesunate, a

derivative of artemisinin is frequently used to treat mild to severe malaria (Cen et al., 2018). Besides its antimalarial effects, artesunate has been shown to exert anticancer properties (Khanal, 2021). Many studies demonstrated that artesunate and other artemisinin derivatives significantly enhance the impact of radiation on lung cancer, cervical cancer, and human glioma cells (Zhao et al., 2011; Luo et al., 2014; Berte et al., 2016). However, little is known about probable mechanism of artesunate effect on cancer stem cells (CSCs) and hypoxia in cancer patients.

Materials and Methods

This study was done on 8 groups, each group included 8 Ehrlich solid carcinoma (ESC) bearing mice as follows, Group I: Untreated ESC bearing mice as control group. Group II: Mice irradiated with single dose of IR (6Gy). Group III: Mice treated with artesunate alone (50mg/kg/day). Group IV: Mice treated with the combination of single dose of IR and artesunate (50mg/kg/day). Group V: Mice treated with artesunate alone (100 mg/kg/day). Group VI:

Mice treated with the combination of single dose of IR and artesunate (100 mg/kg/day). Group VII: Mice treated with artesunate alone (200mg/kg/day). Group VIII: Mice treated with the combination of single dose of IR and artesunate (200mg/kg/day), administration of artesunate was then maintained once daily by oral intubation for 3 consecutive days.

Animals

Adult mice weighing 20-25 g, with an average age of about 10-12 weeks old, were purchased from the animal house of Faculty of Agriculture, Alexandria University. They were kept 8 per cage throughout the experiment and were maintained on a standard laboratory diet and water. In this study, the protocol was in accordance with the National Institutes of Health Guide for the Care and Use of Laboratory Animals. The research was approved by the Research Ethics Committee of the Medical Research Institute, University of Alexandria (AU0122122311).

Transplantation of Ehrlich solid tumors in the mice

A line of Ehrlich Ascites Carcinoma (EAC) cells (obtained from the National Cancer Institute, Cairo University) was transplanted intraperitoneally in female Albino mice. The intraperitoneal fluid containing Ehrlich ascites cells was collected. RBCs in the tumor fluid were disrupted by giving a hypotonic shock with 0.4% NaCl for 15 minutes and centrifuged. The pellet was washed in normal NaCl (0.9%) and resuspended in phosphate buffered saline (PBS). Approximately 2×10^6 cells in 0.2 ml PBS were injected subcutaneously into the right thigh of the lower limb of the mice and allowed to develop into a solid tumor for 10 days.

The tumor volume was measured with a Vernier caliper, and the mice with a palpable solid tumor mass of approximately 100 mm³ were used in the study. Tumor volume and %Tumor inhibition rate were calculated as follows:

Tumor volume $(mm^3) = 1 / 2ab^2$ (where a is the tumor diameter and b is the tumor minor diameter).

%Tumor inhibition rate = $1 - (mean volume of treated tumors) / (mean volume of control tumors) <math>\times 100$

Radiation exposure

Irradiation with X-ray was carried out in a linear accelerator (PRIMUS, Mid-Energy, Toshiba Medical systems, Tokyo, Japan) with X-ray energy outputs of dose rates of 300 Mu/min at Ayadi El-mostakbal Oncology Centre. Animals were subjected to whole body X-irradiation dose of 6 Gy.

Preparation of tissue homogenate

Solid tumors were gathered, washed in ice cold saline, blotted dry, and weighted before being homogenized in 0.2 M phosphate buffer with PH 7.4 (1:9 w/v). Homogenization was done using a glass homogenizer with a loose filling Teflon pestle in an ice bath (4°C). Centrifugation of the homogenates was carried out at 4°C for 10 minutes at 6000 ×g to obtain the supernatant for determination of CD44, ALDH1A1, HIF-1 α and VEGF by ELISA according to the .manufacturer's instructions (cloud clone corp., USA)

Preparation of tumor tissue for histopathology study

Following necropsy, tumor tissues were obtained from different mice groups rinsed in saline solution and then placed at least 24 hours in 10% buffered formalin (pH 7.4). Fixed tissue specimens have been processed using the conventional paraffin embedding technique, sectioned at 4.5 μ m and stained with Mayer's hematoxylin and eosin stain. Stained sections were examined by light microscope (Leica DM500) and photographed using a digital camera (Leica EC3, Leica, GmbH, Wetzlar, Germany).

Immunohistochemistry

Paraffin-embedded tissue sections were prepared. According to the manufacturer's protocol, deparaffinized retrieved tissue sections were treated by 0.3% $\rm H_2O_2$ for 20 Minutes. Then were incubated with anti P53 (Abcam-ab131442- 1:100) at 4°C overnight. Then washed out by PBS followed by incubation with secondary antibody HRP Envision kit (DAKO) 20 minutes; washed out and incubated with diaminobenzidine (DAB) for 15 minutes. Washed by PBS then counter staining with hematoxylin, dehydrated and clearing in xylene then cover slipped for microscopic examination.

Stained sections were examined by light microscope (Leica DM500) and photographed using a digital camera (Leica EC3, Leica, GmbH, Wetzlar, Germany). Photomicrographs were processed and analyzed for counting the number of P53 immunostained cells using the Image J. software version 1.36 (National Institutes of Health, USA).

Determination of hypoxia markers in tumor tissue homogenate using ELISA

Hypoxic markers, VEGF and HIF- 1α concentrations were measured in tumor tissue homogenate samples, using ready to use ELISA kits (Mouse hypoxia-inducible factor 1α , HIF 1α ELISA Kit cloud clone corp., USA) and (Mouse vascular endothelial growth factor, VEGF ELISA Kit cloud clone corp., USA), according to manufacturer's instruction.

Determination of stemness markers in the tumor tissue homogenate using ELISA

Stemness markers, CD44 and ALDH1A1 levels were measured in tumor tissue homogenate samples, using ready to use ELISA kits (Mouse cluster of differentiation, CD44 ELISA Kit, cloud clone corp., USA) and (Mouse Aldehyde Dehydrogenase 1 Family Member A1, ALDH1A1 ELISA kit, cloud clone corp., USA) according to manufacturer's instruction.

Statistical analysis

The statistical analysis was done using IBM SPSS software package version 20. (Armonk, New York: IBM Corp). The Kolmogorov-Smirnov test was used to verify the normality of distribution. Quantitative data was described by mean values & standard error. One-way ANOVA followed by Tukey's multiple comparison test was used to evaluate the significant differences among the treatment groups. The significance of the obtained results was judged at the 5% level.

Results

Impact of Artesunate and IR treatment on tumor volume and tumor inhibition rate

For all studied groups, the average tumor volume and tumor inhibition rate are illustrated in Tables 1 and 2 and Figure 1. Following the treatment of artesunate and/or ionizing radiation, a significant decrease in the tumor volume was noticed, showing a synergistic suppressing effect. The tumor inhibition rate was elevated significantly after administration of artesunate at doses of 50, 100, and 200 mg/kg alone or in combination with IR as compared to the IR treated mice.

Impact of Artesunate and IR treatment on tissue CD44, ALDH1A1, HIF-1 α and VEGF

Statistical analyses of tissue CD44 (pmol/L), ALDH1A1 (ng/L), HIF-1 α (ng/ml) and VEGF (pg/ml) in all the studied groups are presented in Table 3. CD44 showed insignificant difference between the treated groups and untreated groups except groups treated with 200mg/kg ART alone or in combination with single dose of IR (6Gy) were significantly increased (<0.001 respectively). p1=0.008, ALDH1A1 significantly increased in groups treated with either artesunate alone or in combination with single dose of IR (6Gy) compared to untreated group. However, insignificant difference was found between IR only treated group and untreated control (p1=0.863). $HIF-1\alpha$ showed insignificant difference between the treated groups with either IR, ART alone or in

combination with IR when compared to untreated control group.

VEGF showed significant increase in treated groups with either ART alone or in combination with IR when compared to untreated control group. While there was no significant difference found between IR alone treated group and untreated control group (p1=0.999).

Impact of Artesunate and radiation treatment on apoptotic cells number

Statistical analysis of apoptotic cells number in each studied group is shown in Table 4. IR alone, ART alone with different concentrations and combination treatment of both IR and ART significantly increase the number of apoptotic cells when compared to untreated control. Combination of ART and IR significantly increase the number of apoptotic cells in concentration dependent manner compared to IR only treated group.

Impact of Artesunate and radiation treatment on P53 immunostained cells

Statistical analysis of P53 immunostained cells in all studied groups are illustrated in Table 5 and representative photograph of ESC sections taken from different studied groups are shown in Figure 2. P53 immunostained cells significantly increased in groups treated with either artesunate alone or in combination with IR compared to untreated group while, insignificant difference was found between group treated with IR only and untreated group (p1= 0.432). Combination of artesunate and IR significantly increase the P53 immunostained cells in a concentration dependent manner when compared to IR only treated group.

Histopathological results

Control ESC showed completely viable solid tumors composed of sheets of large polygonal, round, hyperchromatic polymorphic malignant cells with unusual giant morphologies. Several degrees of nuclear and cellular pleomorphism were seen and very few numbers of apoptotic and necrotic cells were identified (Figure 3A). ESC treated with ionizing radiation showed remnants of tumor cells and areas of diffuse necrosis (Figure 3B). ESC treated with 50 mg /kg of artesunate showed a slight increase in the number of apoptotic tumor cells characterized as pycnotic nuclei with basophilic cytoplasm associated with focal areas of necrosis (Figure 3C). Similarly, ESC treated with 100 mg/kg of artesunate showed degenerated areas of tumor with a marked increase in the number of apoptotic and focal areas of necrosis (Figure 3E). However, more apoptotic tumor cells, regression of tumor cell invasion and focal areas of necrosis were observed in ESC treated with ART 200 mg/kg of artesunate (Figure 3G).

Table 1. Tumor volume (mm³) in all studied groups.

Groups	Tumor vo		
Groups	0 day	3 rd day	P
Control	232.0 ± 41.97	345.66±36.11	0.001*
IR (6 Gy)	262.25 ± 42.43	195.88 ± 35.97	0.019*
ART (50mg/kg)	268.63 ± 66.62	170.56 ± 58.58	0.015*
ART (50mg/kg) + IR	125.26 ± 20.86	76.20 ± 18.14	0.004*
ART (100mg/kg)	261.75 ± 46.81	133.19 ± 18.15	0.004*
ART (100mg/kg) + IR	368.44 ± 46.69	223.19 ± 29.63	0.004*
ART (200mg/kg)	204.88 ± 29.42	100.06 ± 27.41	<0.001*
ART (200mg/kg) + IR	218.69 ± 29.99	73.45 ± 13.50	<0.001*

p: p-value for comparing between 0 day and 3rd day in each group. *: Statistically significant at p < 0.05

Table 2. Tumor inhibition rate in all studied groups.

	Control	IR (6 Gy)	ART (50mg/kg)	ART (50mg/kg) + IR	ART (100mg/kg)	ART (100mg/kg) + IR	ART (200mg/kg)	ART (200mg/kg) + IR
Tumor inhibitionrate (%) Mean ± SE	0.0±0.0	17.39±4.16	44.16±9.04	44.32±7.63	45.21±5.08	33.14±6.92	58.46±8.04	60.94±10.5
p1		0.015*	0.001*	0.001*	<0.001*	0.009^{*}	<0.001*	<0.001*
p2			0.031*	0.041^{*}	0.038*	0.023*	0.003*	0.001*
р3			0.97	73	(0.367	0.	830

p1: p-value for comparing between Control and each other group. p2: p-value for comparing between IR and each other group. p3: p-value for comparing ART and ART + IR at different concentrations. *: Statistically significant at p < 0.05. SE: Standard error. Control: Untreated EC bearing mice. ART: Artesunate. IR: EC-bearing mice treated with single dose of ionizing radiation (6 Gray).

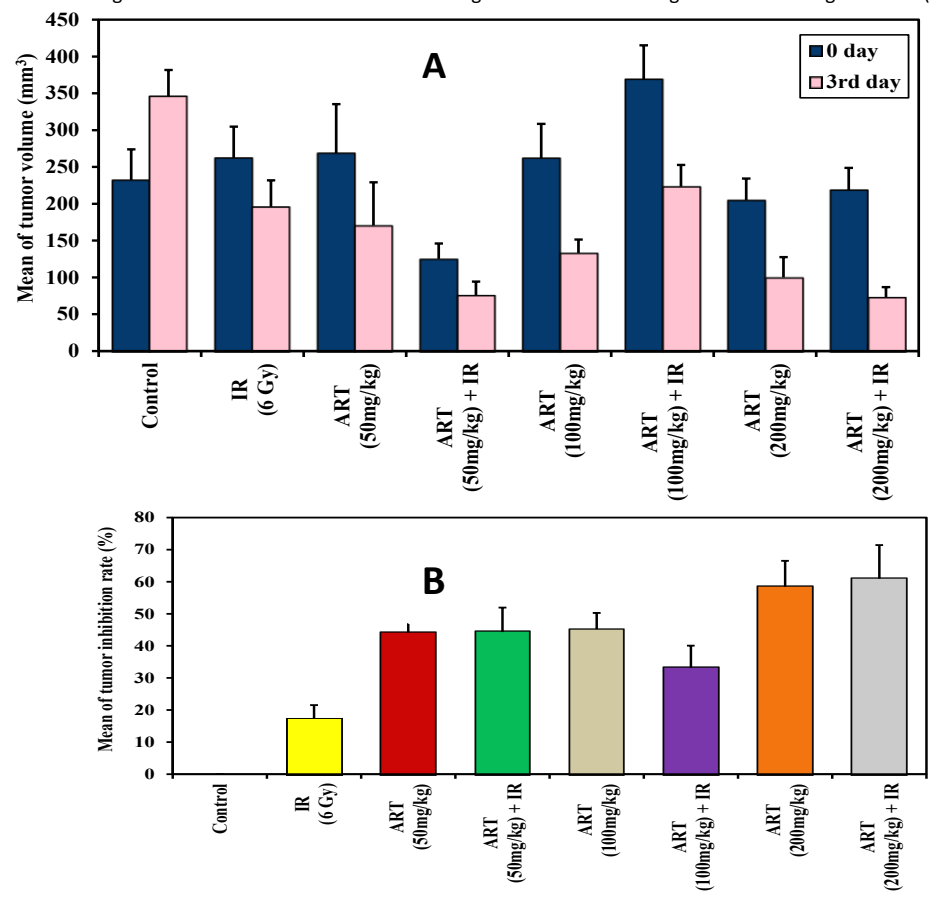


Figure 1. A) Bar chart representing the mean values of tumor volume at the beginning of the experiment and after 3 days in all studied groups; B) Bar chart depicts the mean values of tumor inhibition rate in all studied groups. Control: Untreated EC bearing mice ART: Artesunate

Table 3. Statistical analyses of CD44 (pmol/L), ALDH1A1 (pg/ml), HIF-1α (ng/ml) and VEGF (pg/ml) in all studied groups

	Control	IR (6 Gy)	ART (50mg/kg)	ART (50mg/kg) + IR	ART (100mg/kg)	ART (100mg/kg) + IR	ART (200mg/kg)	ART (200mg/kg) + IR
CD44 Mean ± SE	361.7±9.55	332.1±13.62	340.0±4.42	361.7±4.54	367.9±5.62	392.0±6.85	414.4±11.53	436.8±15.31
p ₁		0.397	0.762	1.000	1.000	0.374	0.008*	<0.001*
p ₂			0.999	0.400	0.179	<0.001*	<0.001*	<0.001*
p ₃			0.765		0.659		0.734	

ALDH1A1 Mean ± SE	102.1±3.15	115.0±1.81	143.6±2.66	130.2±9.09	139.5±3.74	188.7±12.59	171.7±7.17	176.1±4.42	
p ₁		0.863	0.001*	0.069	0.004*	<0.001*	<0.001*	<0.001*	
p ₂			0.060	0.726	0.164	<0.001*	<0.001*	<0.001*	
p₃			0.8	35	<0.0	001*	1.0	000	
HIF-1α Mean ±SE	26.46 ± 1.76	28.94 ± 4.64	30.81 ± 3.65	32.04 ± 2.03	85.89±5.40	62.60 ± 1.21	65.27 ± 4.66	75.85 ± 1.83	
p1		1.000	1.000	1.000	0.010*	0.865	0.816	0.571	
p ₂			1.000	1.000	0.013*	0.902	0.862	0.633	
p ₃				1.000		0.284		1.000	
VEGF Mean ± SE	1393.9±30.2	1370.1±22.7	1469.3±18.1	1552.0±34.5	1605.0±32.5	1602.7±27.0	1725.6±17.1	1883.4±31.1	
p ₁		0.999	0.525	0.003*	<0.001*	<0.001*	<0.001*	<0.001*	
p ₂			0.192	<0.001*	<0.001*	<0.001*	<0.001*	<0.001*	
p ₃				0.404		1.000		0.003*	

 p_1 : p-value for comparing between control and each other group.

 ${\bf Control: Untreated \ EC \ bearing \ mice.}$

ART: Artesunate.

IR: ESC treated with single dose of ionizing radiation (6 Gray).

 Table 4. Statistical analysis of apoptotic cells number in all studied groups.

	Control	IR (6 Gy)	ART (50mg/kg)	ART (50mg/kg) + IR	ART (100 mg/kg)	ART (100mg/ kg) + IR	ART (200mg/ kg)	ART (200mg/ kg) + IR
Apoptotic cells Mean ±SE	4.35 ± 0.58	11.33 ± 1.59	17.94 ± 1.42	20.89 ± 1.16	25.69 ± 1.47	32.06 ± 1.51	34.11 ± 2.22	40.52 ± 1.94
p ₁		0.046*	<0.001*	<0.001*	<0.001*	<0.001*	<0.001*	<0.001*
p ₂			0.070	<0.001*	<0.001*	<0.001*	<0.001*	<0.001*
p₃			0.877		0.092		0.088	

p1: p-value for comparing between Control and each other group.

Control: Untreated EC bearing mice

ART: Artesunate

IR: ESC treated with single dose of ionizing radiation (6 Gray).

 p_2 : p-value for comparing between IR and each other group.

 p_3 : p-value for comparing ART and ART + IR at different concentrations.

^{*:} Statistically significant at p < 0.05.

SE: Standard error.

p2: p-value for comparing between IR and each other group.

p3: p-value for comparing ART and ART + IR at different concentrations.

^{*:} Statistically significant at p < 0.05

SE: Standard error

 Table 5. Statistical analyses of P53 immunostained cells in all studied groups.

	Control	IR (6 Gy)	ART (50mg/kg)	ART (50mg/kg) + IR	ART (100mg/kg)	ART (100mg/kg) + IR	ART (200mg/kg)	ART (200mg/kg) + IR
P53 Mean ± SE	6.40 ± 0.93	13.07 ± 1.47	18.57 ± 1.19	23.20 ± 3.06	27.90 ± 1.87	36.14 ± 1.51	41.21 ± 3.41	53.48 ± 3.07
p ₁		0.432	0.008*	<0.001*	<0.001*	<0.001*	<0.001*	<0.001*
p ₂			0.670	0.046*	<0.001*	<0.001*	<0.001*	<0.001*
p ₃			0.829		0.183		0.007*	

p1: p-value for comparing between Control and each other group.

p2: p-value for comparing between IR and each other group.

p3: p-value for comparing ART and ART + IR at different concentrations.

*: Statistically significant at p < 0.05

SE: Standard error

Control: Untreated EC bearing mice

ART: Artesunate

IR: ESC treated with single dose of ionizing radiation (6 Gray).

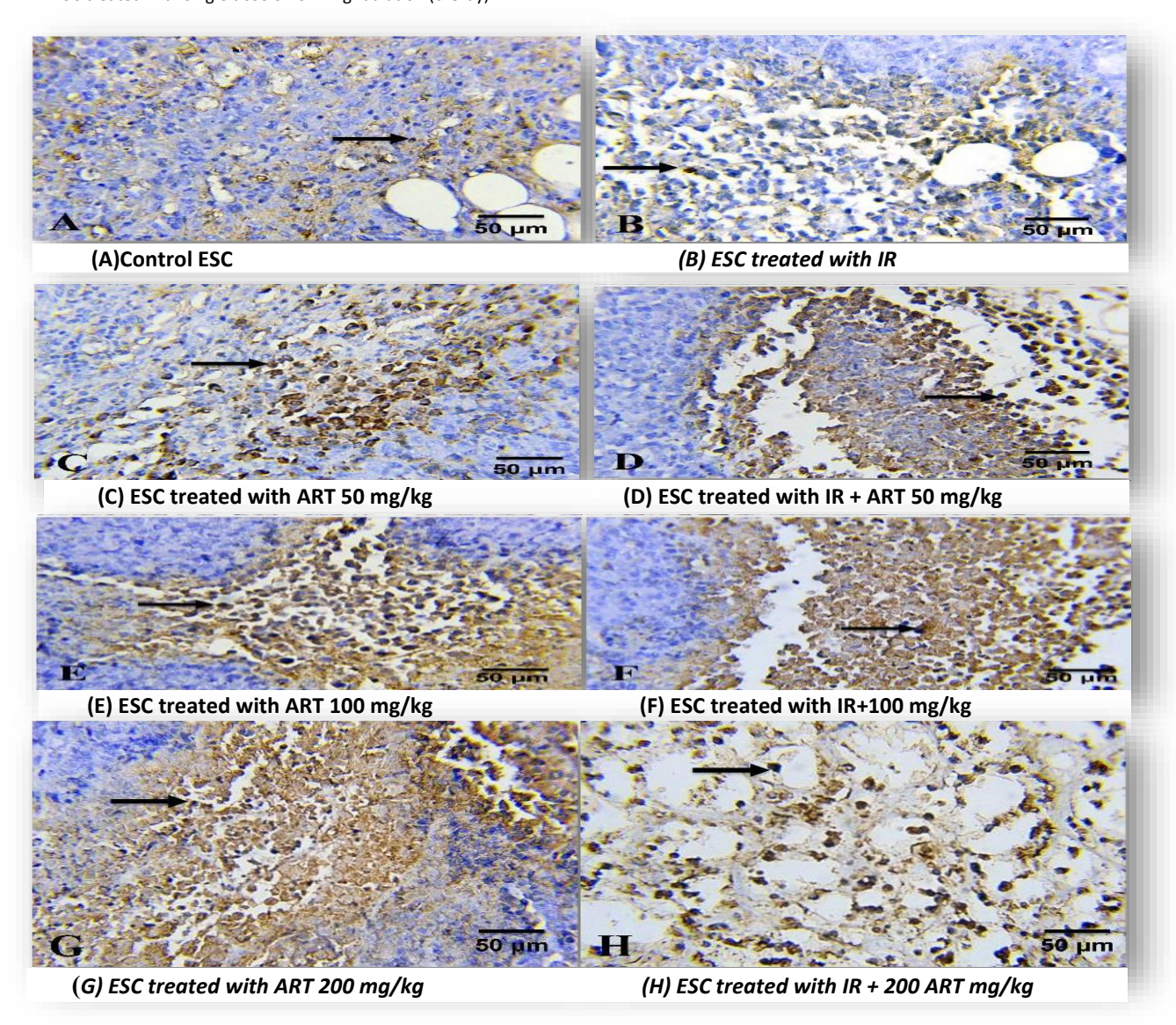


Figure 2. Representative photomicrograph of ESC sections taken from the different studied groups and (IHC, ×400). Black arrow represents P53 immunostained cells.

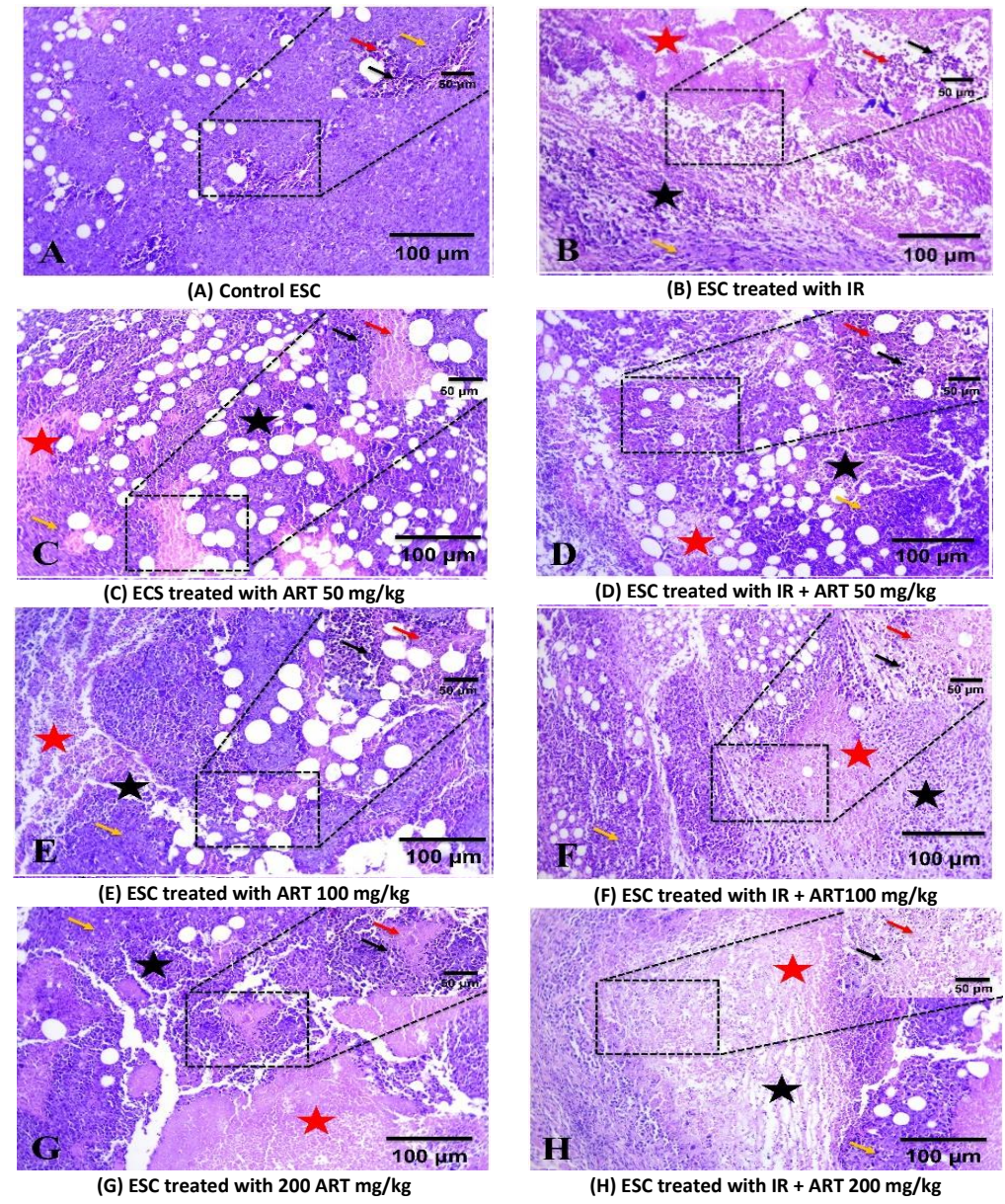


Figure 3. Representative photomicrograph of ESC sections taken from the different studied groups and stained by H&E at magnification powers 100 and 400. Pleomorphic tumor cell (yellow arrow), necrotic tumor cell (red arrow), apoptotic cell (black arrow), area of necrosis (red star) area of apoptosis (black star).

Following treatment of ESC with ionizing radiation in combination with 50 mg/kg of artesunate (Figure 3D), 100 mg/kg (Figure 3F) and 200 mg/kg (Figure 3H) respectively exhibited large eras of necrosis and apoptotic ESC cells with pyknotic nuclei and inflammatory cells and regenerative eosinophilic cytoplasm cells with vesiculated nuclei. However, ESC treated with ART 200 mg/kg showed the most noticeable effect in tumor regression.

Discussion

Artesunate derived from artemisinin is an antimalarial drug and has been identified as an efficient radiosensitizer in several studies. Recent studies have shown that, artesunate has anti-tumor

activity via inhibiting tumor cell migration, proliferation, and cell cycle arrest (Chen et al., 2019; Zhao et al., 2020). However, little is known about the effects of artesunate on cancer stem cells (CSCs) and hypoxia in cancer. The current study was conducted to evaluate the radio sensitization of artesunate by targeting stemness and hypoxia on Ehrlich solid tumor. The present study showed that artesunate and single dose of IR (6Gy) alone or in combination has a potential synergistic suppressive and cytotoxic effect against ESC in a dose dependent manner, where a significant pronounced effect was demonstrated in the tumor volume following treatment of ESC with artesunate in combination with single dose of IR (6Gy). Therefore, the present

findings supported the previously demonstrated suppressive and cytotoxic effects of artesunate in human cancer cell lines (Augustin et al., 2015; Yang et al., 2019). In agreement with previous in vivo study demonstrated that, the tumor volume in the artesunate treated group had significantly reduced (Wang et al., 2017).

Radiosensitizers are substances that exhibit enhanced tumor inactivation when combined with radiation therapy compared to the cumulative effect of each modality (Metselaar et al., 2021). Moreover, the present study revealed that combining different doses of artesunate with single dose of IR (6Gy) significantly increase ionizing radiation induction of tumor damage reflected by increase tumor inhibition rate in comparison to radiation only treated ESC. This result demonstrated that artesunate enhanced the radiosensitivity in the animal model. The maximum inhibition rate was observed when 200 mg/Kg of artesunate was combined with a single dose of IR (6Gy). Histopathological examination of ESC stained with H&E further confirmed these results, ESC treated with a single dose of IR (6Gy) showed only areas of diffuse necrosis and remnants of tumor cells. Following treatment of ESC with single dose of IR (6Gy) in combination with Artesunate 50 mg/kg, 100 mg/kg and 200 mg/kg respectively exhibited large eras of necrotic and apoptotic ESC cells with pyknotic nuclei and inflammatory cells and regenerative eosinophilic cytoplasm cells with vesiculated nuclei. However, the most noticeable effect in tumor regression was observed with artesunate 200 mg/kg suggesting the radiosensitizing effect of artesunate.

Our result is supported by Fei et al in vivo study on esophageal cancer who showed that, when mice were treated with both ionizing radiation and artesunate, the tumor volume increased at a much slower rate than when the mice were treated with ionizing radiation alone (Fei et al., 2018). Targeting apoptotic pathways is still a promising cancer therapeutic strategy that will continue to advance in future clinical practice (Carneiro and El-Deiry, 2020). Our results demonstrated that the apoptotic effect against tumors in ESC treated with artesunate alone, ionizing radiation alone or in combination is dosedependent, where combining different doses of artesunate with ionizing radiation significantly increases apoptotic cells number in comparison to radiation only treated mice. These results demonstrate that artesunate may trigger apoptosis of the transplanted tumor and enhance ionizing radiation-induced apoptosis in a dose-dependent manner. Consistent with the results of the present study Liu et al reported that the percentages of apoptotic cells in esophageal cancer increased with increasing artesunate concentration (Liu et al., 2015). In addition to previous studies indicated that artesunate suppresses the growth of human breast cancer cells MCF-7 (Jamalzadeh et al., 2017), gastric cancer cells (Wang et al., 2017) and colon cancer cells (Jiang et al., 2018) by inducing apoptosis. However, Zhou et al. (2013) showed that artesunate suppressed gastric cancer proliferation via oncosis rather than apoptosis.

An indispensable role of p53 throughout the body is maintaining DNA stability and preventing cancer (Berke et al., 2022). p53 is the transcription factor that stimulates the expression of DNA repair proteins in response to DNA damage. When the damage is severe, p53 induces apoptosis by expressing apoptosis-related genes. p53, is a vital factor in inhibiting cellular carcinogenesis and killing cancer cells by induction of apoptosis (Hibino and Hiroaki, 2022). The present data confirmed the apoptotic effect against tumors where a significant gradual increase was found in the expression of p53 after treatment of ESC with artesunate alone, single dose of IR (6Gy) alone or in combination when comparing with that of untreated ESC. Whereas combining different doses of artesunate with IR significantly increases the expression of p53 in comparison to that in single dose of IR (6Gy) only treated mice.

These results indicated that, artesunate triggered apoptosis of tumor cells by improving the expression of apoptotic gene p53. This finding agrees with the result of Longxi et al. (2011) who demonstrated that artesunate has the potential to increase the expression of p53, with a significant elevation seen as the drug concentration increases. On the other hand, previous study demonstrated that inducing apoptosis mediated by artesunate was not p53-dependent (Dong, & Wang, 2014) which contradicts our finding.

As a clinically and biologically important phenomenon, hypoxia is intensively studied particularly in cancer. In the large arteries' wall, the primary source of oxygen and nutrients for the cells on the luminal side is luminal blood diffusion, while perfusion through vasa vasorum supplies nutrients to the cells on the abluminal side. A hypoxic microenvironment is generated by any change in these processes, or an alteration in oxygen consumption by cells (Grossmannova et al., 2022).

As regards hypoxic markers in the present study, the statistical analyses of our data revealed insignificant difference in all comparisons concerning the tissue homogenate HIF- 1α , but the statistical analyses of VEGF revealed a significant elevation in the concentration of VEGF in ESC treated with

artesunate alone or combined with single dose of IR (6Gy). These results give evidence that artesunate induces hypoxia and this effect is often temporary. Acute hypoxia is often caused by acute hemolysis, which lowers the oxygen content in the blood (Machogu and Machado, 2018). It has been demonstrated that artesunate accumulates in three major tissues, the erythrocytes, the liver, and kidney (Li et al., 2005). After accumulation of artesunate in the erythrocytes, causes the generation of ROS because of iron heme species found in red blood cells splitting its endoperoxide bridge (O'neill et al., 2010). Although a moderate level of ROS has beneficial effects, excessive generation may be damaging to human cells, particularly erythrocytes (Salman et al., 2017). The artesunate-induced lipid peroxidation seen with short-term LDA treatment in both genders is consistent with prior studies indicating that artesunate-induced hemolysis is facilitated by the production of free radicals (Shittu et al., 2013).

Patients with anemia symptoms may require cautious administration of artesunate, with doses and durations are relatively moderate, due to the increased risk of hemolysis that may become apparent with prolonged oral artesunate use. Coadministration of artesunate with exogenous antioxidants, such as vitamins C and E, is highly recommended and potential drug users should also be warned about artesunate-induced hypoglycemia and hemolysis/anemia as possible side effects (Salman et al., 2017).

In contrast with our results previous studies showed that in EOMA cells treated with artesunate, VEGF-A, VEGFR-2, and HIF-1 α levels were decreased significantly in a time-dependent manner (Wang et al., 2017). This contradict may be due to our study is in vivo study while Wang et al. (2017) is in vitro study.

Cancer stem cells (CSCs) are a subset of cancer cells that promote tumor initiation and progression. Regarding self-renewal and differentiation, CSCs are resembled to normal stem cells. To detect CSCs, several cell surface markers have been identified, which are elevated in different malignancies (Vasefifar et al., 2022). Hypoxia has been demonstrated to promote the expression of stem cell markers in several malignant cell types such as glioblastoma (Bar et al., 2010), breast cancer (Conley et al.,2012) and neuroblastoma (Mohlin et al., 2017). Regarding stemness markers in the current study, the statistical analyses of our data revealed that insignificant difference in the levels of CD44 and ALDH1A1 between the ESC treated with single dose of IR (6Gy) and untreated mice. ESC treated with artesunate alone or in combination with single dose of IR (6Gy) showed insignificant difference when

compared to untreated mice, but administration of artesunate at high concentration 200mg/kg alone or in combination with single dose of IR (6Gy) significantly increase the stemness markers CD44 and ALDH1A1. These results indicated that, antitumor and radiosensitivity effect of artesunate are stemness independent. In previous study, Chen et al. (2020) initially investigated the impact of artesunate on the stemness of leukemia cells. Their findings demonstrated that artesunate inhibited the stemness of leukemia cells, as shown by reduced expressions of stem cell marker proteins such as CD44, SOX2, ALDH1, and OCT4, and confined sphere formation (Chen et al., 2020). This study contradicts our findings.

Conclusion

Artesunate enhanced radiosensitivity of ESC by increasing apoptotic cells and increasing the expression of P53. Artesunate induces the hypoxia, and this effect is often temporary due to artesunate inducing hemolysis of RBCs via free radical generation. Artesunate should be handled with caution in patients with symptoms of anemia as possibility of hemolysis.

Future investigation is needed to explore the potential clinical use of artesunate as a chemotherapeutic agent for breast cancer and other cancers are needed as well as to characterize the radiosensitive mechanisms of artesunate.

Author Contribution Statement

Mohamed I. Morsi interpreted the study results and participated in manuscript writing. Sanaa A. El-Benhawy presented the research proposal idea, performed the practical part of the study and contributed to writing the manuscript. Samar S. Elblehi collected the histopathological tissue samples and examined the histological slides. Osama O. Almesrati shared the idea in research proposal, participated in the practical work and results interpretation and manuscript writing. Amal R.R. Arab participated in the practical work, results interpretation and manuscript writing.

Funding

The study is self-funded.

Ethics approval

This study was approved by the Institutional Animal Care and Use Committee (IACUC)-Alexandria University. The research also follows the ARRIVE guidelines and the National Research Council's guide for the care and use of laboratory animals.

Acknowledgements

All authors read and approved of the final manuscript.

Availability of data

Data presented in the study and any related data are available upon request.

Conflict of Interest

No conflict of interest is declared.

References

- Augustin, Y., Krishna, S., Kumar, D., & Pantziarka, P. (2015). The wisdom of crowds and the repurposing of artesunate as an anticancer drug. Ecancermedicalscience, 9, ed50.
- Bar, E. E., Lin, A., Mahairaki, V., Matsui, W., & Eberhart, C. G. (2010). Hypoxia increases the expression of stemcell markers and promotes clonogenicity in glioblastoma neurospheres. The American journal of pathology, 177(3), 1491-1502.
- Berke, T. P., Slight, S. H., & Hyder, S. M. (2022). Role of Reactivating Mutant p53 Protein in Suppressing Growth and Metastasis of Triple-Negative Breast Cancer. OncoTargets and therapy, 15, 23-30.
- Berte, N., Lokan, S., Eich, M., Kim, E., & Kaina, B. (2016). Artesunate enhances the therapeutic response of glioma cells to temozolomide by inhibition of homologous recombination and senescence. Oncotarget, 7(41), 67235-67250.
- Carneiro, B. A., & El-Deiry, W. S. (2020). Targeting apoptosis in cancer therapy. Nature reviews. Clinical oncology, 17(7), 395-417.
- Cen, Y. Y., Zao, Y. B., Li, P., Li, X. L., Zeng, X. X., & Zhou, H. (2018). Research progress on pharmacokinetics and pharmacological activities of artesunate. Zhongguo Zhong yao za zhi= Zhongguo Zhongyao Zazhi= China Journal of Chinese Materia Medica, 43(19), 3970-3978.
- Chen, H., Tao, J., Wang, J., & Yan, L. (2019). Artesunate prevents knee intraarticular adhesion via PRKR-like ER kinase (PERK) signal pathway. Journal of Orthopaedic Surgery and Research, 14(1), 448.
- Chen, S., Gan, S., Han, L., Li, X., Xie, X., Zou, D., & Sun, H. (2020). Artesunate induces apoptosis and inhibits the proliferation, stemness, and tumorigenesis of leukemia. Annals of Translational Medicine, 8(12), 767.
- Conley, S. J., Gheordunescu, E., Kakarala, P., Newman, B., Korkaya, H., Heath, A. N., ... & Wicha, M. S. (2012). Antiangiogenic agents increase breast cancer stem cells via the generation of tumor hypoxia. Proceedings of the National Academy of Sciences, 109(8), 2784-2789.
- Dong, H. Y., & Wang, Z. F. (2014). Antitumor effects of artesunate on human breast carcinoma MCF-7 cells and IGF-IR expression in nude mice xenografts. Chinese Journal of Cancer Research, 26(2), 200-207.
- Fei, Z., Gu, W., Xie, R., Su, H., & Jiang, Y. (2018). Artesunate enhances radiosensitivity of esophageal cancer cells by inhibiting the repair of DNA damage. Journal of Pharmacological Sciences, 138(2), 131-137.

- Goswami, N., Luo, Z., Yuan, X., Leong, D. T., & Xie, J. (2017). Engineering gold-based radiosensitizers for cancer radiotherapy. Materials Horizons, 4(5), 817-831.
- Grossmannova, K., Barathova, M., Belvoncikova, P., Lauko, V., Csaderova, L., Tomka, J., ... & Madaric, J. (2022). Hypoxia Marker Carbonic Anhydrase IX Is Present in Abdominal Aortic Aneurysm Tissue and Plasma. International Journal of Molecular Sciences, 23(2), 879.
- Hibino, E., & Hiroaki, H. (2022). Potential of rescue and reactivation of tumor suppressor p53 for cancer therapy. Biophysical Reviews, 14(1), 267-275.
- Jamalzadeh, L., Ghafoori, H., Aghamaali, M., & Sariri, R. (2017). Induction of apoptosis in human breast cancer MCF-7 cells by a semi-synthetic derivative of artemisinin: a caspase-related mechanism. Iranian journal of biotechnology, 15(3), 157-165.
- Jiang, F., Zhou, J. Y., Zhang, D., Liu, M. H., & Chen, Y. G. (2018). Artesunate induces apoptosis and autophagy in HCT116 colon cancer cells, and autophagy inhibition enhances the artesunate-induced apoptosis. International journal of molecular medicine, 42(3), 1295-1304.
- Jiang, W., Li, Q., Xiao, L., Dou, J., Liu, Y., Yu, W., ... & Wang, J. (2018). Hierarchical multiplexing nanodroplets for imaging-guided cancer radiotherapy via DNA damage enhancement and concomitant DNA repair prevention. ACS nano, 12(6), 5684-5698.
- Khanal, P. (2021). Antimalarial and anticancer properties of artesunate and other artemisinins: current development. Monatshefte für Chemie, 152(4), 387-400
- Li, Q., Xie, L. H., Si, Y., Wong, E., Upadhyay, R., Yanez, D., & Weina, P. J. (2005). Toxicokinetics and hydrolysis of artelinate and artesunate in malaria-infected rats. International journal of toxicology, 24(4), 241-250.
- Liu, L., Zuo, L. F., Zuo, J., & Wang, J. (2015). Artesunate induces apoptosis and inhibits growth of Eca109 and Ec9706 human esophageal cancer cell lines in vitro and in vivo. Molecular Medicine Reports, 12(1), 1465-1472.
- Longxi, P., Buwu, F., Yuan, W., & Sinan, G. (2011). Expression of p53 in the effects of artesunate on induction of apoptosis and inhibition of proliferation in rat primary hepatic stellate cells. PLoS One, 6(10), e26500.
- Luo, J., Zhu, W., Tang, Y., Cao, H., Zhou, Y., Ji, R., & Cao, J. (2014). Artemisinin derivative artesunate induces radiosensitivity in cervical cancer cells in vitro and in vivo. Radiation oncology, 9(1), 84.
- Machogu, E. M., & Machado, R. F. (2018). How I treat hypoxia in adults with hemoglobinopathies and hemolytic disorders. Blood, 132(17), 1770-1780.
- Metselaar, D. S., du Chatinier, A., Stuiver, I., Kaspers, G. J., & Hulleman, E. (2021). Radiosensitization in Pediatric High-Grade Glioma: Targets, Resistance and Developments. Frontiers in Oncology, 11,662209.
- Mohlin, S., Wigerup, C., Jögi, A., & Påhlman, S. (2017). Hypoxia, pseudohypoxia and cellular differentiation. Experimental Cell Research, 356(2), 192-196.
- O'neill, P. M., Barton, V. E., & Ward, S. A. (2010). The molecular mechanism of action of artemisinin—the debate continues. Molecules, 15(3), 1705-1721.

- Salman, M. T., Ajayi, P. O., Alagbonsi, A. I., & Olatunji, L. A. (2017). Artesunate-induced hemolysis and hypoglycemia in rats: gender implication and role of antioxidant enzymes. Journal of Applied Hematology, 8(1), 23-32.
- Seigel, R. L., Miller, K., & Jemal, A. (2020). Cancer statistics, 2020. A cancer journal for clinicians, 70(1), 7-30.
- Shittu, S. T., Oyeyemi, W. A., Okewumi, T. A., & Salman, T. M. (2013). Role of oxidative stress in therapeutic administration of artesunate on sperm quality and testosterone level in male albino rats. African Journal of Biotechnology, 12(1), 70-73.
- Vasefifar, P., Motafakkerazad, R., Maleki, L. A., Najafi, S., Ghrobaninezhad, F., Najafzadeh, B., ... & Baradaran, B. (2022). Nanog, as a key cancer stem cell marker in tumor progression. Gene, 827, 146448.
- Wang, L., Liu, L., Wang, J., & Chen, Y. (2017). Inhibitory effect of artesunate on growth and apoptosis of gastric cancer cells. Archives of Medical Research, 48(7), 623-630.
- Wang, N., Chen, H., Teng, Y., Ding, X., Wu, H., & Jin, X. (2017). Artesunate inhibits proliferation and invasion of mouse hemangioendothelioma cells in vitro and of tumor growth in vivo. Oncology letters, 14(5), 6170-6176.
- Xu, Q., Zhang, H., Liu, H., Han, Y., Qiu, W., & Li, Z. (2022). Inhibiting autophagy flux and DNA repair of tumor cells to boost radiotherapy of orthotopic glioblastoma. Biomaterials, 280, 121287.
- Yang, Y., Wu, N., Wu, Y., Chen, H., Qiu, J., Qian, X., ... & Zhuang, J. (2019). Artesunate induces mitochondriamediated apoptosis of human retinoblastoma cells by upregulating Kruppel-like factor 6. Cell death & disease, 10(11), 1-12.
- Zhang, X. D., Luo, Z., Chen, J., Song, S., Yuan, X., Shen, X., ... & Xie, J. (2015). Ultrasmall glutathione-protected gold nanoclusters as next generation radiotherapy sensitizers with high tumor uptake and high renal clearance. Scientific reports, 5, 8669.
- Zhao, F., Vakhrusheva, O., Markowitsch, S. D., Slade, K. S., Tsaur, I., Cinatl, J.,. & Juengel, E. (2020). Artesunate Impairs Growth in Cisplatin-Resistant Bladder Cancer Cells by Cell Cycle Arrest, Apoptosis and Autophagy Induction. Cells, 9(12), 2643.
- Zhao, Y., Jiang, W., Li, B., Yao, Q., Dong, J., Cen, Y., & Zhou, H. (2011). Artesunate enhances radiosensitivity of human non-small cell lung cancer A549 cells via increasing NO production to induce cell cycle arrest at G2/M phase. International immunopharmacology, 11(12), 2039-2046.
- Zhou, X., Sun, W. J., Wang, W. M., Chen, K., Zheng, J. H., Lu, M. D., ... & Zheng, Z. Q. (2013). Artesunate inhibits the growth of gastric cancer cells through the mechanism of promoting oncosis both in vitro and in vivo. Anti-Cancer Drugs, 24(9), 920-927.